Porous InP as Piezoelectric Matrix Material in 1-3 Magnetoelectric Composite Sensors

M.-D. GERNGROSS*, M. LEISNER, J. CARSTENSEN and H. FÖLL
Institute for Materials Science, Christian-Albrechts-University of Kiel,
Kaiserstrasse 2, 24143 Kiel, Germany
* *mdg@tf.uni-kiel.de*

***Abstract* – This work shows the results of the fabrication of semi-insulating piezoelectric porous InP structures by electrochemical etching and subsequent purely chemical post–etching in an isotropic HF, HNO_3, EtOH and HAc containing electrolyte. The piezoelectric modulus d_{14} of porous InP is measured to around |60| pm / V, which larger by a factor of 30 compared to bulk InP.**

***Index Terms* – indium phosphide, porous, piezoelectricity, magnetoelectric sensor.**

I. INTRODUCTION

This paper focuses on the production of an effective and cheap piezoelectric material for the application in magnetoelectric 1-3 composite sensors. The concept is to apply porous and piezoelectric InP as the matrix material. In the second step a multilayer stack consisting of NiFe / FeGa showing giant magnetostrictive behavior will be used as magnetostrictive filler.

The 1-3 composite arrangement of piezoelectric and magnetostrictive materials is chosen, because it allows for very large contact areas, providing excellent mechanical coupling between both components, and thus high sensitivity to magnetic fields.

The main characteristic of piezoelectric materials is the lack of an inversion center. InP as a III-V compound semiconductor belongs to the $4,\bar{3}3m$ cubic crystal system. This crystal class is non centro-symmetric and non-polar. Thus InP is piezoelectric, but not pyroelectric. Looking at the piezoelectric modulus tensor of InP reveals that the d_{14} component is the only remaining component of the piezoelectric modulus tensor [1]. The maximum piezoelectric effect is calculated to be in the <100> direction.

The piezoelectric properties of bulk InP have only been measured very rarely [2, 3]. Up to now InP has not been used as piezoelectric material, because it is not possible to produce intrinsic InP. Even highly pure InP contains a lot of impurities, which serve as doping centers, so that a large number of free charge carriers exist short-circuiting the charges induced by the piezoelectric effect.

To overcome this problem, our approach is to produce a self-organized, hexagonally closed packed array of so-called current-line pores with completely overlapping space charge regions (SCR). Inside the space charge regions hardly any free charge carriers are present, so that the induced polarization by the piezoelectric effect will not be shortened anymore.

II. EXPERIMENTAL

For the experiments only single crystalline, double-side polished (100) InP wafers are used. The wafers are doped with S with a carrier concentration of $N_D = 1.1 \cdot 10^{17}$ cm^{-3}. The resistivity is 0.019 Ωcm. The wafer thickness is 500 µm ± 10 µm. The sample size is $A = 0.25$ cm^2.

All electrochemical etching experiments have been performed in the electrochemical double-cell as described elsewhere [4]. The electrochemical etching has been performed under potentiostatic conditions at a constant temperature of 20 °C. For the first second a voltage pulse of 15 V is applied to the sample in order to obtain a homogenous pore nucleation. It is followed by a constant etching potential of 7 V for 70 min. Afterwards the samples are carefully rinsed in deionized water and blown dry in nitrogen.

The purely chemical post-etching is carried out in a plastic beaker at room temperature. The post-etching electrolyte consist of HF : HNO_3 : EtOH : HAc (3 : 8 : 15 : 24). In this etching solution, the hydrofluoric acid serves as an etching agent, nitric acid as an oxidizing agent, and ethanol and acetic acid as wetting agents. The ethanol also serves as a passivating agent in order to decrease the etching speed.

The samples are purely chemical post-etched for various times from 8 h to 48 h to investigate the etching properties of the etchant. After the post-etching process the samples are carefully rinsed in deionized water and blown dry in nitrogen.

The etched porous InP nanostructures have been investigated with a HELIOS D477 SEM. The piezoelectric response to an applied voltage has been measured with a double beam laser interferometer (DBLI) from aixACCT.

III. RESULTS & DISCUSSION

Figure 1 (a) presents the InP current-line pore structure after anodic electrochemical etching ($U > 0$ V) with adjacent mechanical polishing to remove the nucleation layer, which was performed for imaging and comparing the resulting pore structures after different chemical treatments. This structure is the result of the anodic electrochemical etching process optimized to produce hexagonally closed packed pore arrays in a self-organized manner.

During the anodic electrochemical etching process the minimum distance between pore walls is assumed to be twice the width of the space charge region. At the end of the electrochemical etching process, the externally applied voltage by the potentiostat is to a value determined by the surface charges. Hence the width of the space charge region shrinks and thus the remaining conductive areas, where no space charge region is present, increase. These conductive

areas can only be reduced if the pore wall width is reduced to twice the length of the SCR at cell off conditions. This can be achieved by performing a post-etching step. The post-etching electrolyte has to be isotropic over the complete pore length and should be self-limiting as soon as the space charge regions of neighboring pores overlap again. As post-etching electrolyte an HF : HNO_3 : EtOH : HAc (3 : 8 : 15 : 24) containing electrolyte has been developed. The pore structure resulting from post-etching in this electrolyte is shown in Fig. 1 (b).

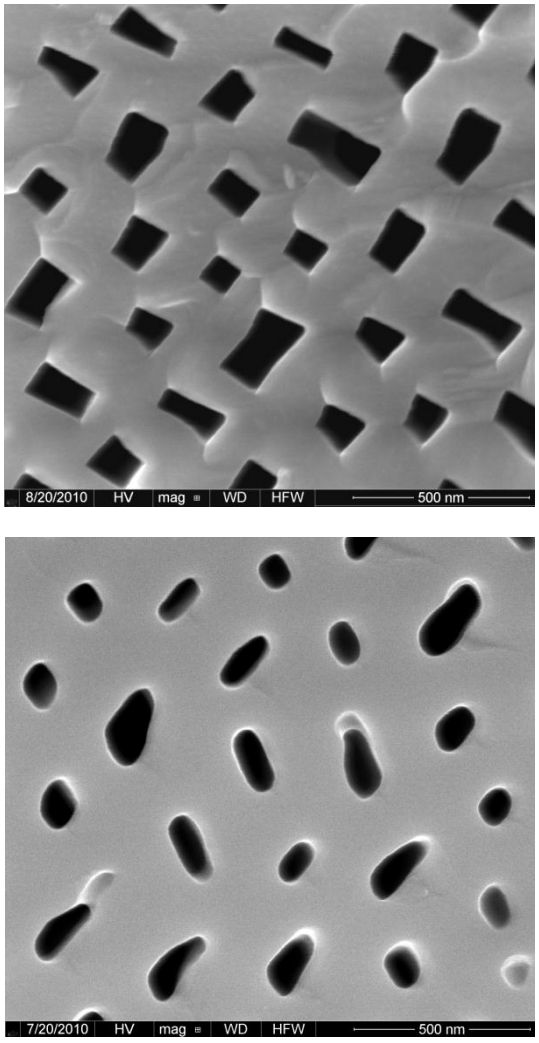

(a)

(b)

Fig. 1 Top view of porous InP (a) after anodic electrochemical etching (U > 0 V) and (b) after subsequent purely chemical post-etching (U = 0 V) after 48 h.

Comparing both pore structures, one observes that the pores change their shape from rectangular / square-like after the anodic electrochemical etching to elliptic /circular after subsequent post-etching for 48 h. This etching behavior is only possible for isotropic etchants.

Looking at the distances between the pores, one recognizes that the pore wall width of two neighboring square-like resp. circular pores is mostly the smallest measured in the SEM images shown, while for two neighboring rectangular like resp. elliptical pores oriented parallel to each other is the largest found in the majority of the cases.

Figure 2 (a) shows the pore-ratio as a function of the etching time in the post-etching electrolyte. The pore ratio is the ratio of the longitudinal and the transverse side of the rectangular resp. elliptical pores. It is a quantitative measure for the change in the shape of the rectangular pores as a result of the post-etching. Fig. 2 (a) shows an increasing pore-ratio in the range from 0 h to 28 h of post-etching from around 1.7 for the not post-etched sample to a level in the range of 2.35, reached after approximately 28 h of post-etching. The pore-ratio of the samples, being etched for 8 h and 16 h in the post-etchant respectively, deviates from the red line. A possible explanation for this could be that the etch rate is higher for the surface near part of the pores in the beginning of the post-etching process, but drops to zero after twice the width of the SCR is reached.

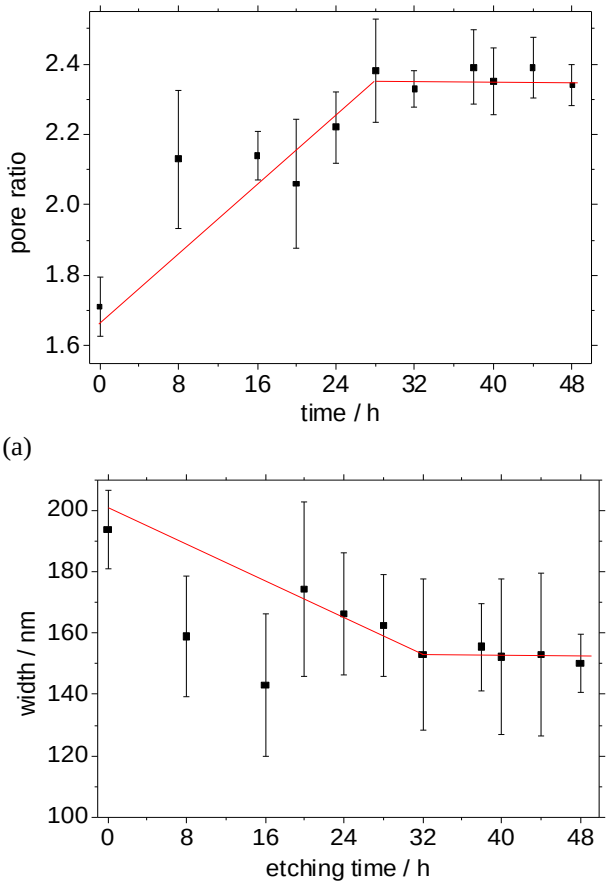

(a)

(b)

Fig. 2 (a) pore ratio as a function of the etching time in the post-etching electrolyte and (b) mean width of the pore walls as a function of the post-etching time in the post-etching electrolyte.

Fig. 2 (b) shows the average pore wall width as a function of the etching time in the post-etching electrolyte.

The mean pore wall width is decreasing from around 190 nm of the not post-etched sample to a level in the range of 150 nm. Again the mean pore wall width for the samples being post-etched for 8 h and 16 h deviate from the red line, possibly due to the same reason as given for the pore ratio, because the mean pore wall width of these two samples fits to the mean pore wall width of samples being post-etched for a much longer time.

The level of 150 nm is reached after approximately 32 h of post-etching and does not change with increasing post-

etching time. This indicates the self-limiting behavior of the post-etching electrolyte.

This result is consistent with the result obtained in the analysis of the pore-ratio of these samples, because an increased pore-ratio goes along with a smaller mean pore wall width. The saturation value of both quantities is reached approximately at the same time, as one can see from the diagrams shown in Figure 2 (a) and 2 (b).

The characteristic change in the pore geometry can be understood by considering the space charge region surrounding each pore, the resulting voltage drop across the SCR and the crystal-orientation dependence of the electrochemical and chemical etching in InP. The pores are expanding in all directions, until an overlap of SCR of neighboring pores occurs, which allows no further dissolution of the InP by the post-etchant.

Figure 3 (a) and (b) show the result of the DBLI measurement of the only electrochemically etched and the electrochemically etched sample with additional post-etching. The DBLI measures the displacement of the InP sample due to the piezoelectric effect as a function of the voltage, which is externally applied in <100> direction of the sample via two micromanipulators.

As InP is not a ferroelectric material, one expects a linear dependence of the applied voltage on the measured displacement. The chemical post-etching of the electrochemically etched samples reduces the leakage currents to a level low enough to use the piezoelectric properties. In general, the expected piezoelectric performance of the sample is better, the lower the leakage currents are.

For the only electrochemically etched sample the voltage is linearly increased from 0 V to 3 V, then linearly decreased to –3 V and finally increased to 0 V again. For the electrochemically etched and additionally post-etched sample the voltage is linearly increased from 0 V to 0.5 V, then linearly decreased to –0.5 V and finally increased to 0 V again. The resulting displacement of the InP sample is measured.

Figure 3 (a) shows the piezoelectric performance of the only electrochemically etched sample. In the voltage range, where the applied voltage increases from 0 V to 3 V, one observes a linear behavior of the resulting displacement until a voltage of 2.5 V is reached. At this position the displacement strongly increases, although the applied voltage remains constant. Decreasing the applied voltage to 1.65 V also causes an increase in the displacement, though the displacement is expected to decline for a decreasing voltage. In the voltage range from 1.65 V to -3 V the expected linear behavior is observed and again in the range from -3 V to 0 V. That the ending displacement of the displacement/voltage curve is not equal to the starting displacement of 0 nm is most probably due to dielectric losses, which increase with the frequency of the applied voltage. The slope d_{av} of the linear fit of the displacement / voltage curve is 0.078 nm / V. From the slope of the linear displacement vs. applied voltage curve, the d_{14} component of the porous InP sample can be derived, resulting in a value of |19| pm / V.

As shown in figure 3 (a) it is now possible to fabricate nanostructures in InP by electrochemical etching, where the leakage currents do not completely short the induced polarization by the piezoelectric effect. Although the displacement/voltage curve is not completely linear over the entire voltage range, the d_{14} component of the only electrochemically etched sample is already larger by a factor of about 10 compared to the d_{14} component of bulk InP [5].

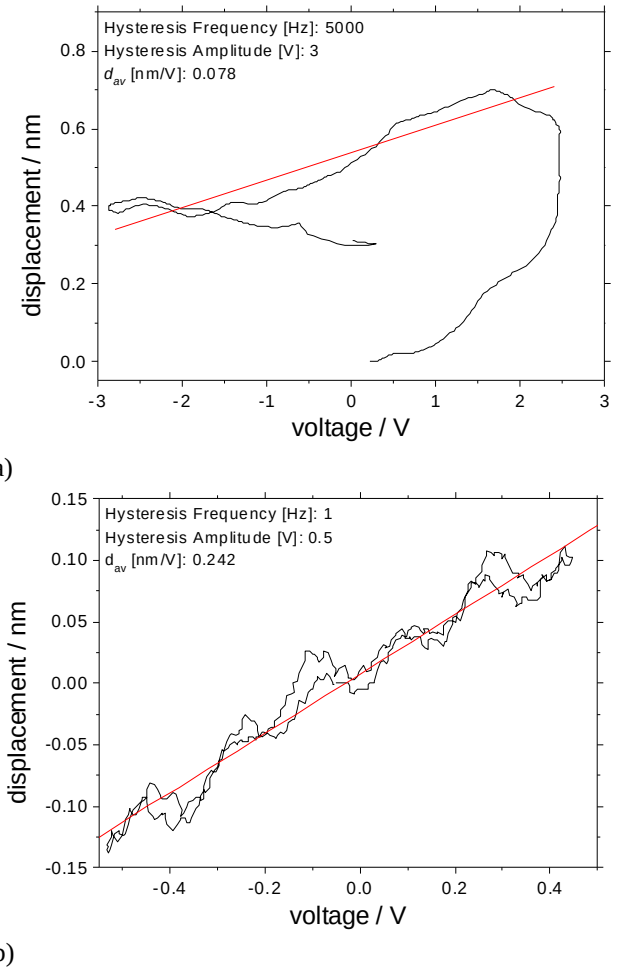

Fig. 3 DBLI measurement of porous InP (a) after anodic electrochemical etching ($U > 0$ V) and (b) after subsequent purely chemical post-etching ($U = 0$ V) after 48 h. The slope of the linear fit is denoted as d_{av}.

Figure 3 (b) shows the piezoelectric performance of the electrochemically etched and subsequently post-etched sample. One obtains a linear dependence of the applied voltage on the measured displacement. In contrast to the purely electrochemically etched sample the positive limit of the applied voltage is reached completely. But more eye-catching is the wavy shape of the displacement/voltage curve of the sample. The waviness of the curve is an artifact of specimen mounting.

The sample exhibits a significantly higher slope with d_{av} = 0.242 nm / V compared to the only electrochemical etched sample. The linear dependence of the applied voltage on the displacement has been measured severeal times with a variation in d_{av} by a factor of 2 in maximum.

It is found to be around |60| pm/V, about a factor of 30 larger than the values measured on bulk InP [5].

IV. CONCLUSION

The first steps on the way to a magnetoelectric 1-3 composite sensor consisting of a piezoelectric matrix and a magnetostrictive filler have been made.

It has been demonstrated that it is possible to produce semi-insulating piezoelectric InP by anodic electrochemical etching and subsequent purely chemical post-etching in an HF, HNO3, EtOH, HAc containing electrolyte. This electrolyte has been optimized to show an isotropic and self-limiting etching behavior over the complete pore length.

The d_{14} component of post-etched macroporous InP is found to be around |60| pm/V, which is about a factor of 30 larger than the values reported for bulk InP [5].

Though InP is the most suitable candidate for this approach, in principle a new class of semi-insulating porous single-crystalline piezoelectric materials can be fabricated from III-V semiconductors by this concept of electrochemical and pure chemical post-etching.

ACKNOWLEDGMENTS

This work was funded by the collaborative research center 855 “Magnetoelectric Composites – Future Biomagnetic Interfaces” by the DFG.

REFERENCES

[1] J.F. Nye, Physical properties of crystals: their representation by tensors and matrices, Oxford University Press, Oxford (1985).

[2] K. Rottner, R. Helbig, and G. Müller, Appl. Phys. Lett. 62(4), 352 (1993).

[3] G. Arlt and P. Quadflieg, Phys. Stat. Sol. 25, 323-330 (1968).

[4] S. Langa, I.M. Tiginyanu, J. Carstensen, M. Christophersen, and H. Föll, Electrochem. Solid-State Lett. 3(11), 514 (2000).

[5] T.P. Pearsall, Properties, processing and applications of indium phosphide, IEEE, London (2000).